Advances in
Bridge Engineering

TECHNICAL NOTE Open Access

Human-induced vibration assessment of a steel arch footbridge with tapered truss cross-section

Matteo Marra[1], Emma Ghini[1*], Giada Gasparini[1] and Stefano Silvestri[1]

*Correspondence:
emma.ghini2@unibo.it

[1] Department of Civil, Chemical, Environmental, and Materials Engineering - DICAM, University of Bologna, Bologna, Italy

Abstract

The serviceability of pedestrian bridges may be affected by the discomfort due to vibrations felt by the users crossing the deck. Design guidelines recommend avoiding critical frequency ranges and provide acceptance criteria for maximum accelerations to assess user discomfort for serviceability conditions. The paper presents selected results from an experimental campaign on a two-hinged steel arch pedestrian bridge, analysing its dynamic response to both ambient and human-induced vibrations. Activities such as walking, running, and jumping are investigated. In this field, many research works are available in the scientific literature, but the vibration analysis of a steel arch footbridge with tapered truss cross-section is still missing. The first six vibration modes of the bridge are identified using the Frequency Domain Decomposition technique, while damping ratios are estimated through Enhanced Frequency Domain Decomposition. Walking and running tests reveal a small shift in the bridge's forced response frequencies compared to its free response. Jumping tests are analysed by isolating specific modal responses and estimating modal damping ratios based on free vibration data after the jump. The study also compares the maximum vertical accelerations recorded during these tests with the acceptance limits provided by technical standards. Overall, the paper provides insight into the vibration assessment of a steel arch footbridge with tapered truss cross-section and offers practical indications for field-data interpretation, as well as reference values of natural frequencies, damping ratios and accelerations for this common kind of infrastructures.

Keywords: Steel arch footbridge, Dynamic identification, Human-induced vibration, Pedestrian comfort assessment, Acceleration acceptance criteria

1 Introduction

Human-induced dynamic excitation of structures and infrastructures, in both vertical and lateral directions, can arise from activities such as walking, running, jumping, and dancing (Bachmann and Ammann 1987). These activities can generate significant dynamic loads and accelerations on slender and lightweight structures – typically made of steel, such as pedestrian bridges – which may trigger a dangerous resonant response of the structure (associated with Ultimate Limit States, ULS), as well as cause discomfort to users (associated with Serviceability Limit States, SLS).

Generally, walking and running activities can be characterized by pacing rate of around 2–3 Hz, respectively, by forward speed around 1.5 m/s for normal walk and 3.3 m/s for jogging, and by time function of the loading composed of sinusoidal functions (Bachmann and Walter 1987; Setra 2006). In this regard, to avoid resonance phenomena, technical codes and guidelines suggest designing pedestrian structures in such a way to move the fundamental frequencies out of critical ranges. For instance, risk frequencies from many articles and regulations are collected in Table 1.2 by Setra (2006), that, on average, identifies the range 1.6–2.4 Hz as the most critical for vertical vibrations. This is basically confirmed by the JRC Technical and Scientific Report (Heinemeyer et al. 2009) which states that, for vertical and longitudinal vibrations, the critical range for natural frequencies of footbridges are 1.25–2.3 Hz (due to the 1st harmonic of pedestrian loads) and 2.5–4.6 Hz (due to the 2nd harmonic of pedestrian loads), whilst, for lateral vibrations, the critical range is 0.5–1.2 Hz (being only affected by the 1st harmonic of pedestrian excitation).

The discomfort that can arise crossing the decks of a footbridge is not only of a physical nature, but also of a psychological one. In fact, the perception of vibrations is intimately linked to symptoms of structural inadequacy and to uncertainty feeling. Acceptance criteria for footbridges are therefore related to the pedestrian comfort, which basically refers to serviceability conditions. As reported by Dallard et al. (2001), who discussed the case-study of the London Millennium footbridge that experienced unexpected large pedestrian-induced lateral vibrations, current acceptance criteria have been derived from experimental subjective tests, mostly in terms of accelerations. Vertical acceleration limits, mainly based on subjective tests for frequencies above 1 Hz, typically range from 0.5 to 1.0 m/s^2. Criteria for lateral motion are less established, but acceleration values between 0.2 and 0.4 m/s^2 are considered appropriate. Heinemeyer et al. (2009) recommend four comfort classes for the design of footbridges: maximum comfort for vertical accelerations smaller than 0.5 m/s^2, medium comfort for vertical accelerations in the range 0.5–1.0 m/s^2, minimum comfort for an acceleration range 1.0–2.5 m/s^2, where 2.5 m/s^2 is considered as the unacceptable discomfort limit. Being more restrictive, Eurocode 0 (EN 1990) recommends maximum values of vertical acceleration, for any part of the deck, equal to 0.7 m/s^2. Furthermore, for the specific case of vertical vibrations with a frequency of around 2 Hz, technical codes agree on maximum value to be in the range 0.5–0.8 m/s^2 (Setra 2006). However, the acceleration range to be adopted in the verification of pedestrian bridges is not straightforward since their vibrations depend on the natural frequency and on the human-induced vertical motion.

Several critical reviews on the dynamic behaviour of footbridges are available in the scientific literature.

Caetano et al. (2009) explored footbridge vibration design, offering practical guidelines for engineers. Their work underscores the necessity of integrating vibration mitigation strategies during the design phase rather than implementing retroactive solutions.

Cunha et al. (2013) discussed the evolution of dynamic testing and continuous monitoring in bridge applications. They highlighted the shift from forced vibration tests to more efficient ambient and free vibration tests, advancements in accelerometer and data acquisition technology, and the development of noncontact measurement

techniques. They showcased the high accuracy of ambient vibration tests by discussing the Millau Viaduct case, and they highlighted the importance of removing environmental influences in vibration-based damage detection, as demonstrated in the Infante D. Henrique Bridge case study.

Maraveas et al. (2015) provided a comprehensive review of human-induced vibrations in footbridges, focusing on various structural types. Their findings emphasize the need for tailored mitigation measures based on specific bridge geometries and materials. They discuss how pedestrian-induced dynamic forces can lead to significant vibrations, affecting user comfort and structural integrity. The authors highlight the phenomenon of synchronous lateral excitation, where pedestrian movement resonates with the bridge's natural frequencies. To mitigate these vibrations, the paper reviews methods such as implementing tuned mass dampers, which have proven effective in enhancing the dynamic performance of steel arch footbridges.

Understanding pedestrian-induced excitations also necessitates studying human-structure interaction.

Zivanovic et al. (2005) reviewed 200 studies and examined vibration sources, transmission path, and human perception. Humans have been identified as the primary source of vibrations in footbridges, but modelling the dynamic forces induced by crowds remains poorly defined despite recent efforts. The vibration path depends on the mass, damping, and stiffness of the footbridge, with damping being the most uncertain yet critical parameter due to its influence on resonant behaviour. Pedestrians are typically both the receivers and the sources of footbridge vibrations, complicating the assessment of dynamic performance.

Racic et al. (2009) conducted an interdisciplinary review of 270 studies regarding experimental identification and analytical modelling of human walking forces. This study combines biomechanics, by discussing kinematics of human body motion and anthropometry that is based on body segment inertial parameters, and structural engineering, by discussing time-domain and frequency-domain force models for human walking and indirect measurement of human loading through ground reaction forces.

Van Nimmen et al. (2014) assessed existing codes of practice for vibration serviceability of footbridges, questioning their adequacy in accurately predicting human-induced responses. Their findings suggest that many design guidelines may require refinement to better account for real-world pedestrian-structure interactions.

Shahabpoor et al. (2016) conducted a detailed literature review on vertical pedestrian-bridge interactions, shedding light on the complexity of human-induced forces.

Since the infamous prime example of the Millennium Bridge in London (Dallard et al. 2001), numerous case studies on human-induced vibrations in footbridges have been the focus of research, particularly over the past decade, highlighting that this topic still warrants significant attention from the scientific community. Just some examples are cited hereafter.

Da Silva et al. (2018) investigated the dynamic structural behaviour and assessed the human comfort of footbridges when subjected to pedestrian walking, based on the experimental tests performed on a two-span reinforced concrete and steel composite pedestrian bridge located at the Osvaldo Aranha Street in Rio de Janeiro (Brazil). Bridge modal parameters were identified through Operational Model Analysis (OMA) and the

experimental peak accelerations were compared to the recommendations provided by regulations (Setra 2006). The maximum acceleration values (vertical peak accelerations) derived from five walking tests with pedestrian pacing frequencies ranging from 1.6 to 2.45 Hz were found to be in the range of 0.24 m/s^2 to 0.44 m/s^2.

Caetano et al. (2010a, b) developed a comprehensive assessment of the dynamic behaviour of the outstanding Pedro e Inês bridge in Coimbra (Portugal), a steel footbridge consisting of two cantilevered walkways converging at midspan, where each segment structurally supports the other reciprocally, with a deliberate longitudinal misalignment of the two halves. Due to its unique geometry, the bridge was experimentally verified to be prone to vertical and lateral vibrations from pedestrians. Through experimental tests, they identified modal parameters and observed the lateral "lock-in" effect. These findings constituted the basis for the design of a control system based on tuned mass dampers.

Barbosa et al. (2013) examined the dynamic behaviour of the Viana moveable cable-stayed footbridge in Portugal. Dynamic tests, including ambient vibration analysis and pedestrian-induced vibration monitoring, were conducted to assess real-time structural performance over four months. In most cases, accelerations were below 0.5 m/s^2, ensuring maximum comfort. Occasionally, vibrations reached 1 m/s^2 (medium comfort), and sporadically, values between 1–2 m/s^2 (minimum comfort).

Van Nimmen et al. (2021) presented a benchmark dataset on pedestrian-induced vibrations for the Eeklo Footbridge in Belgium. This dataset provides a valuable resource for validating numerical and experimental models used in footbridge vibration analysis.

Li et al. (2023) conducted an experimental and numerical study on the vertical vibrations induced by pedestrians in a glass suspension footbridge. They found that the bridge's low vertical natural frequencies led to resonance during walking and running tests.

The investigation on the dynamic response behaviour of footbridges has also been explored in recent research works through the so-called drive-by monitoring (Feng et al. 2024). Among these, the study from Quqa et al. (2022) addresses the identification of an urban steel bridge for pedestrians and bikes, resulting in the identification of the bridge dynamic features starting from the data collected by sensors integrated in shared mobility.

Among the latest works developed for pedestrian bridge vibration-based identification, Banerjee et al. (2024) proposes a data-driven algorithm for modal parameter identification from output-only video measurements. The methodology, which includes machine learning techniques, such as non-contact video-based modal analysis methods using computer vision techniques has been successfully applied to the historical tapes recording the resonance phenomena that affected the Tacoma Narrows bridge and the London Millennium footbridge.

The reviewed literature underscores the absence of specific vibrational studies dedicated to the structural typology of steel arch pedestrian bridges with the arch below the deck, which could serve as valuable references for both the scientific and professional communities.

The objective of this work is therefore to fill this gap by discussing the case study of a 58-meter-long steel arch footbridge with tapered truss cross-section. This paper includes (i) the dynamic identification and (ii) the assessment of the pedestrian bridge

response to a variety of human-induced vibrations (walking, running and jumping). In detail, this manuscript aims at providing an example of application of in-field dynamic measurements. It covers and conveys practical indications for field-data interpretation, a comparison between the responses induced by different input, and reference orders of magnitude of the deck acceleration responses of this typical kind of steel footbridge, that can be useful for both researchers and practitioners tackling similar problems.

2 The case study: the steel arch footbridge in Pianoro

The case study is the pedestrian bridge in the Savena torrent river park within the municipality of Pianoro in the province of Bologna (Italy), crossing the homonymous river. It was designed according to the Italian technical code (NTC 2018).

The main structure of the pedestrian bridge is a steel two-hinged arch realized with a tubular profile made up of five bolted straight pieces and characterised by a hollow circular cross-section with 800 mm in diameter and 14 mm in thickness (see Fig. 1a and b). The horizontal distance between the two hinges is approximately 58 m. The 2.55 m-wide deck, which is completely above the arch, is constituted by a 15 cm-thick lightly-reinforced concrete slab (specific weight $\gamma = 18$ kN/m^3 and cubic characteristic resistance $R_{ck} = 35$ MPa), and a 5 cm-thick asphalt layer. The lateral edges of the slab are supported by two bolted circular steel tubular profiles with a diameter of 273 mm and a thickness of 6.3 mm. These profiles are connected to the main arch through transversal circular steel tubular profiles with a diameter of 193 mm and a thickness of 6.3 mm, spaced at a constant interval of 2.0 m (see Fig. 1d and e). The abutments (see Fig. 1c) are made of reinforced concrete and rest on foundation piles with a circular cross-section, 800 mm in diameter and 14 m in length. The pedestrian safety barrier consists of a parapet with a steel mesh and vertical uprights.

Despite being similar in appearance, unlike typical deck-arch bridges, e.g. deck-arch bridges with the deck above the arch such as the Porta Westfalica Footbridge in Dortmund (Hajdu 2014), half-through arch bridges like the Ainolanpolku Bridge in Finland, or shallow-arch deck bridges such as the Solferino bridge in Paris, the bridge under investigation is instead conceived with a different design principle. It is configured as an arch bridge with tapered truss cross-section, realised with a single arch-shaped tubular lower chord and a double upper chord realised with two lateral tubular profiles connected by diagonal elements of variable length. The resulting cross-section is a triangular-shaped truss in which the slab is used as a horizontal element that closes the V-shaped structural steel system. Hence, the deck and the arch constitute a unified structural element.

On the contrary, in typical shallow-arch deck bridges, the deck and the arch are two distinct structural elements. The supporting arch, conceived – and also often built – as a self-standing structural element, is partially merged with the deck accommodating the pedestrian traffic, in the proximity of the midspan. Instead, in the remaining portions and in the proximity of the abutments, the arch and the deck are usually connected by vertical elements intended to transmit the load from the deck to the arch. In such structures, indeed, the arch and the deck constitute an interconnected system of independent structural elements.

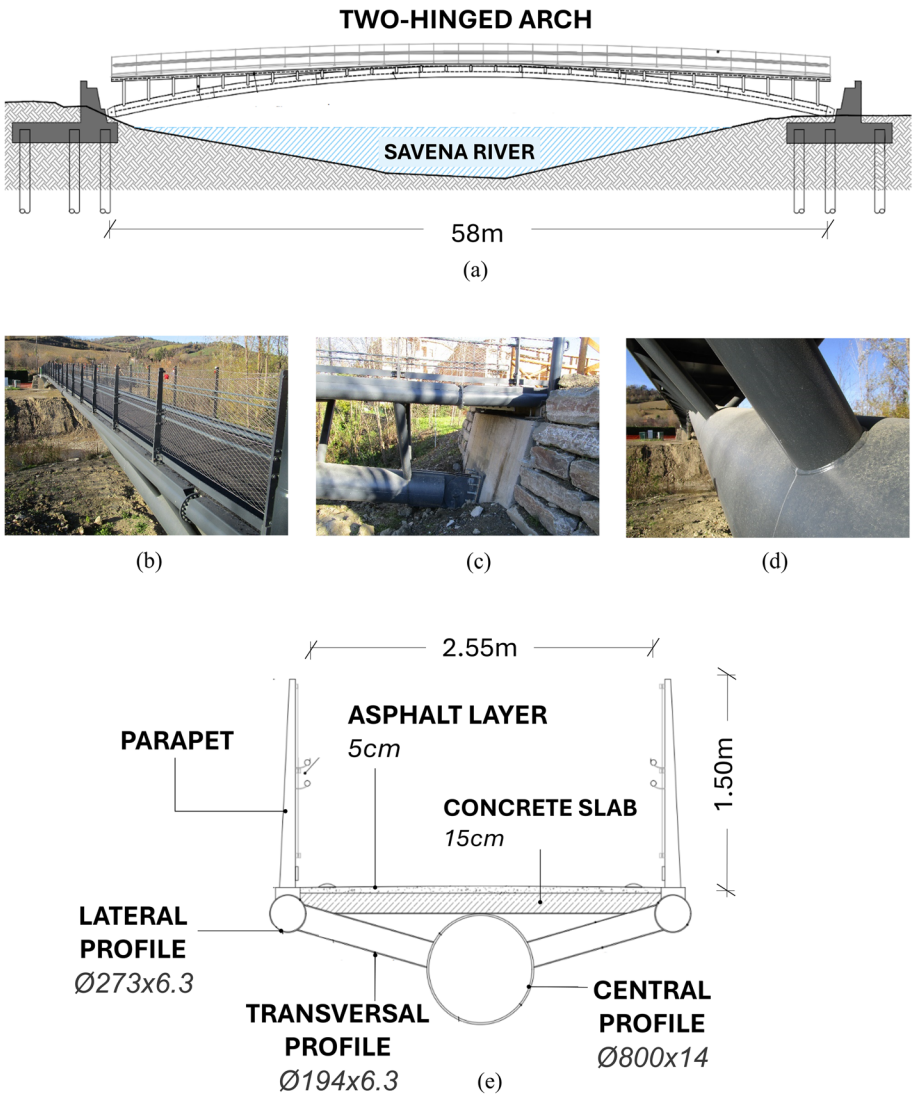

Fig. 1 The pedestrian bridge in Pianoro: (**a**) lateral view, (**b**) bridge deck, (**c**) detail of the abutment, (**d**) detail of the transversal circular steel tubular profiles connecting the deck to the main arch, and (**e**) transversal cross-section at bridge midspan. (All measures, if not specified, are given in [mm])

As an additional distinctive aspect, the selected case study is representative of a design solution used for medium-size span steel footbridges. Despite being used in practical applications, the literature on this bridge category lacks vibrational experimental tests, that could be beneficial for designers in the dynamic response assessment for structural safety and user comfort.

3 The experimental campaign

The pedestrian bridge was built in August 2021 and the experimental campaign was conducted in November 2021. The experimental tests took place under stable weather conditions and in the absence of wind. The temperature recorded during the three testing hours, in proximity to the test location, ranged from 10.5 °C to 11 °C, reflecting

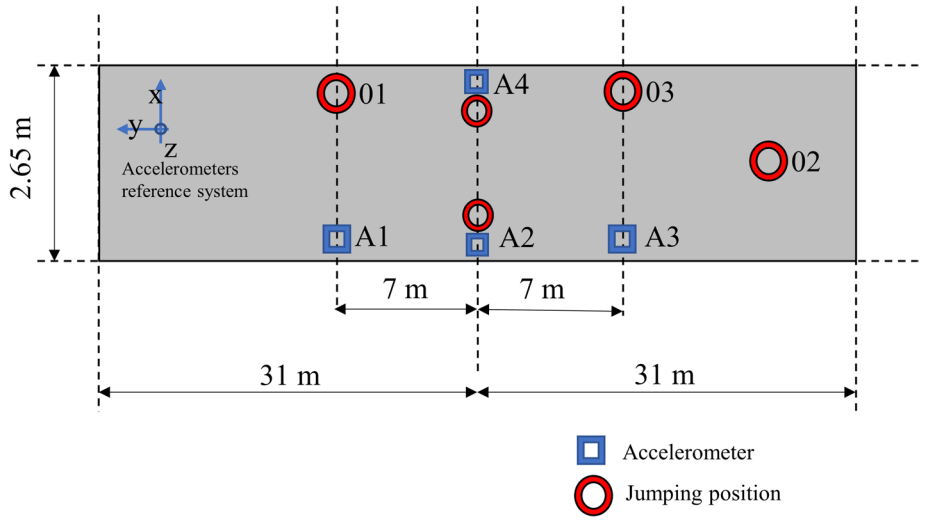

Fig. 2 Schematic view of the bridge deck with accelerometers and jumping positions

negligible effects of environmental factors on the test results. Indeed, as demonstrated by tests conducted on a steel pedestrian bridge in the same area and under similar environmental conditions (Quqa et al. 2022), such small ranges of temperature variation do not perceptibly affect the identification of experimental modal frequencies.

In order to measure the real dynamic response of the pedestrian bridge, two types of dynamic tests were performed: (i) ambient vibration tests, and (ii) human-induced loading tests. During these tests, the accelerations in 4 points of the bridge deck were measured. Figure 2 shows a schematic view of the bridge deck illustrating the positions of the triaxial accelerometers A1, A2, A3 and A4 together with the positions of the jumping tests (see Table 1). The four accelerometers were located in order to capture the main flexural and torsional modes of the bridge. The reference system is organized as follows: X represents the transversal direction, Y represents the longitudinal direction and Z represents the vertical direction.

The dynamic tests were characterized by a sampling frequency equal to 400 Hz with a low-pass filter application at 100 Hz provided by the acquisition system. In the analysis process, since the frequencies of the bridge are below 10 Hz, a decimation procedure has been applied to the accelerations measured during ambient vibration tests in order to reduce the sampling frequency from 400 Hz to 20 Hz. The sampling frequency for the human-induced loading tests has been maintained to 400 Hz since all the samples are needed for a sound identification of the forced dynamic response. The human-induced loadings have been conducted according to different pedestrian traffic situations: (i) walking of 3 and 13 people at fixed frequencies, (ii) running of 3 and 10 people at fixed frequencies, (iii) random use of the bridge (walking and running), and (iv) jumping of 4 people in fixed positions on the bridge deck. Table 1 summarizes the dynamic tests conducted on the pedestrian bridge.

Table 1 Summary of the dynamic tests conducted on the pedestrian bridge

Test category	Test type	Test number	Test description	Test duration [min]
Environmental /randomly man-induced	Random vibration	1	Ambient vibration	15
		2	Random walking and running over the bridge	15
Human-induced	Walking	3	Walking of 3 people at 2 Hz	5
		4	Walking of 13 people at 1 Hz	5
		5	Walking of 13 people at 2 Hz	5
	Running	6	Running of 3 people at 3 Hz	5
		7	Running of 10 people at 3 Hz	5
	Jumping	8	Jump of 4 people in position 03	1
		9	Jump of 4 people in position 03	1
		10	Jump of 4 people in position of the accelerometer A4	1
		11	Jump of 4 people in position of the accelerometer A4	1
		12	Jump of 4 people in position of the accelerometer A1	1
		13	Jump of 4 people in position of the accelerometer A1	1
		14	Jump of 4 people in position 01	1
		15	Jump of 4 people in position 01	1
		16	Jump of 4 people in position 02	1
		17	Jump of 4 people in position 02	1

4 Ambient vibration tests: dynamic identification

The dynamic identification of the modal parameters of the pedestrian bridge has been carried out by means of two output-only identification techniques exploiting the ambient vibration measurements: (i) the Frequency Domain Decomposition (FDD) (Brincker et al. 2000; Brincker and Ventura 2015) and (ii) the Covariance-driven Stochastic Subspace Identification (SSI-Cov) (Peeters and De Roeck 1999; Peeters 2000).

In the application of the two methods, first all channels (encompassing all the three X, Y, Z directions) have been analysed, second only vertical channels (in the Z direction) have been analysed. However, since the difference between the results of the two analyses is negligible and since the main goal was to detect information regarding vertical structural vibration, the results of the second analysis including only the channels of the accelerometers in the vertical direction (Z) are presented.

Within the FDD procedure, the estimation of the spectrum matrix was achieved applying the Welch average (Welch 1967) by dividing the time series of the acceleration signals in segments of 2000 samples (that lead to a frequency resolution of 0.01 Hz) and considering an overlap of 50% between the segments and using Hamming windows to reduce the leakage (Wirsching et al. 2006). After performing the singular value decomposition of that matrix, both singular values and vectors have been identified as a function of the frequency. The SSI-Cov has been applied imposing a time lag for the cross-correlation calculation equal to 7 s and model order in the range 2–50. The corresponding stabilization diagram has been achieved through similitude criteria of 5% for frequency, 5% for damping ratios, and 10% for Modal Assurance Criterion (MAC). Since

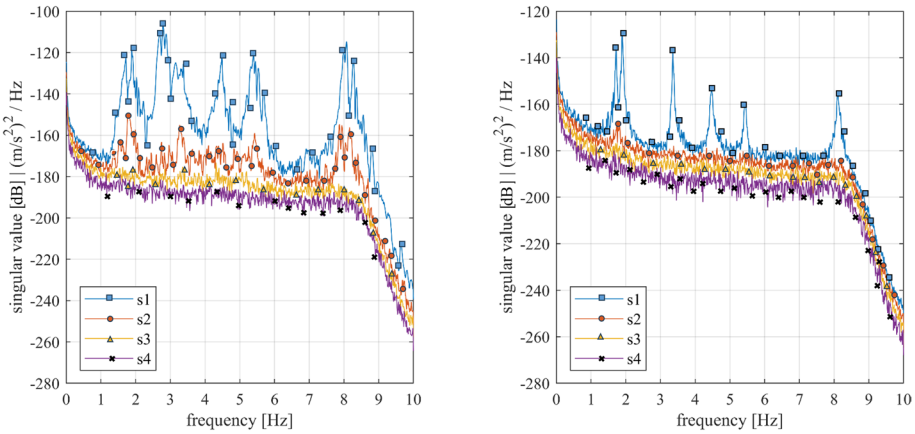

Fig. 3 Singular values spectrum: (**a**) multiple-input loading and (**b**) single-input loading

the FDD and the SSI-Cov methods provide the same results, the stabilization diagram is not reported in this paper and, for the sake of concision, the results reported hereafter only refer to FDD.

The ambient vibration test was performed for a total time of 15 min without interrupting the functionality of the bridge. In general, this can lead to measures affected by multiple – and usually unknown – input loading, due to possible passages of users over the bridge. In this latter case, all singular value curves obtained with the FDD contribute to the modal response of the bridge. On the contrary, if the excitation is a single input only, one singular value curve is significant while the remaining ones are far lower and almost horizontal mainly describing the noise level in the data (Brincker et al. 2003). In this regard, Fig. 3 shows the singular values spectrum from the measured accelerations on the pedestrian bridge obtained for two cases: (i) considering the "as measured" response of the pedestrian bridge (Fig. 3a) thus including multiple-input loading, and (ii) considering the response of the pedestrian bridge deprived of signal parts associated to the external loading due to pedestrians and cyclists crossing the bridge during the acquisition, to maintain only ambient vibration effects (Fig. 3b).

Consequently, Fig. 3b allows to identify six vibration modes whose shapes are estimated taking the singular vectors corresponding to the identified peak frequencies. The identified mode shapes are mainly in the vertical direction and are shown in Fig. 4 (as normalized with respect to their maximum value), while Table 2 reports their corresponding vibration frequency values. In detail, each figure displays both the arch and the deck undeformed profiles, together with four coloured dots indicating the undeformed shape (small dots) and the deformed shape (large dots) of the deck positions where the four accelerometers were located.

The first two flexural mode shapes depicted in Fig. 4a and b appear to be very similar assuming a linear shape in the mid-zone of the deck; they represent the first two theoretical modal shapes of a two-hinged arch in the vertical plane. The third modal shape (Fig. 4c) is also flexural, with the largest displacements in the central part of the arch (quite similar to that of a fully restrained horizontal beam). The fourth mode is torsional; this is clear from the opposite displacement values of accelerometers A2 and A4 (see

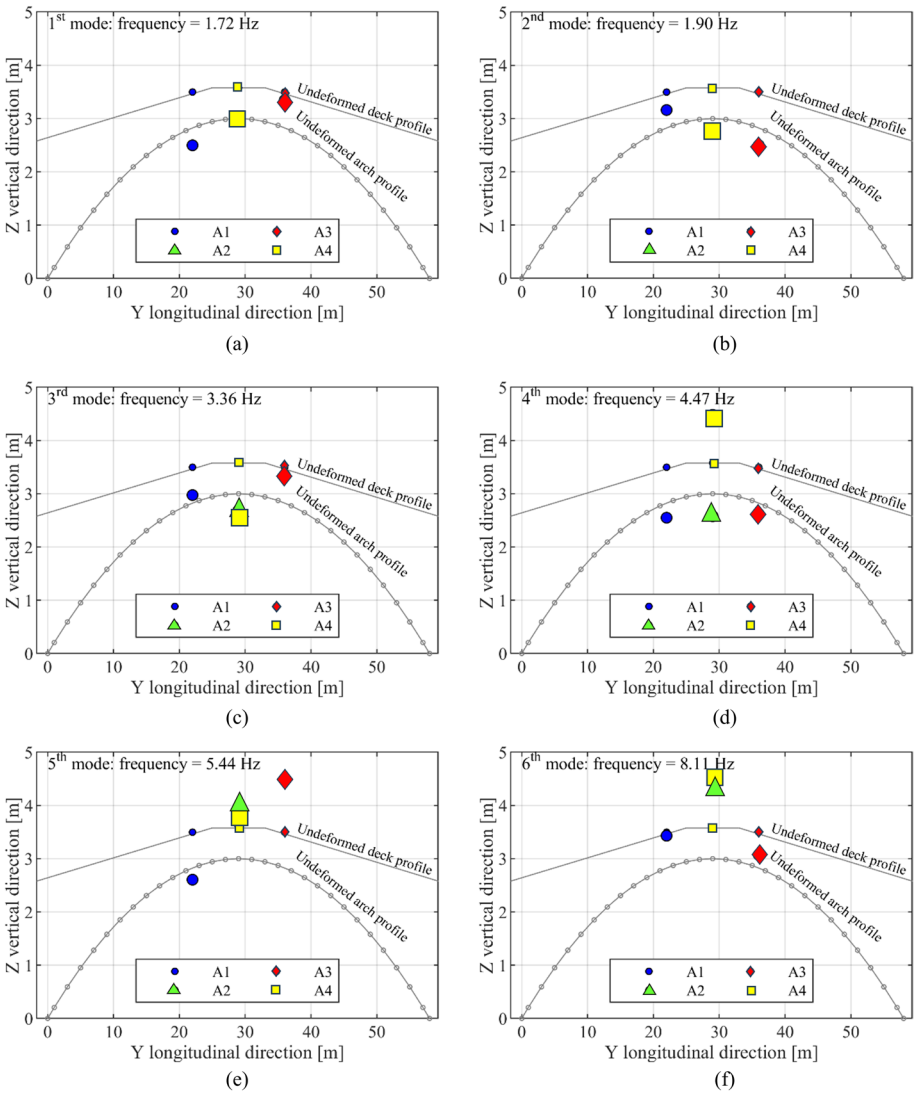

Fig. 4 Identified modal shapes: (**a**) first mode, (**b**) second mode, (**c**) third mode, (**d**) fourth mode, (**e**) fifth mode and (**f**) sixth mode

Table 2 Experimental frequencies and damping ratios of the six identified modal shapes

Mode	FDD	EFDD
	Frequency [Hz]	Damping ratio [%]
1	1.72	0.95
2	1.90	0.90
3	3.36	0.96
4	4.47	0.84
5	5.44	0.71
6	8.11	0.78

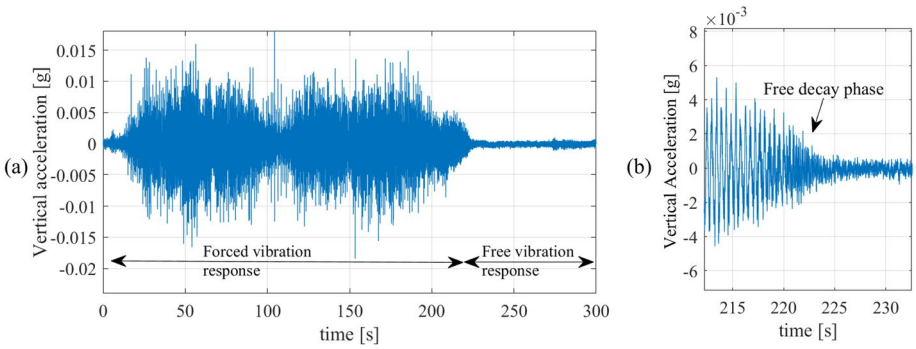

Fig. 5 **a** Vertical acceleration measured during Test #4 for accelerometer A4, with forced and free vibration responses highlighted, (**b**) selected time-window showing the free decay phase illustrating an exponential decay behaviour

Fig. 4d) with respect to the undeformed deck profile. The last two modes appear to be a flexural–torsional coupled one (Fig. 4e) and a high-order flexural one (Fig. 4f). However, due to the low number of accelerometers with respect to the length of the bridge, the estimation of high-order modal shapes is not completely achievable or uniquely determined.

To achieve a first broad identification of the modal parameters of the bridge under consideration, the damping ratios of the identified modes have been estimated. Specifically, damping estimation has been performed with a revised version of the FDD method, known as Enhanced Frequency Domain Decomposition (EFDD), proposed by Brinker et al. (2001). In this work, the EFDD has been applied to the data considering a Modal Assurance Criterion (MAC) rejection level equal to 0.8. The obtained damping ratios are reported in Table 2; they are all around 1%.

5 Human-induced vibration tests: methodology and results

The response of the pedestrian bridge to walking, running and jumping has been investigated by means of analysis and interpretation of the human-induced vibration tests reported in Table 1. For each test, in the vertical acceleration time-history plot, two types of response have been recognised: (i) the forced vibration response and (ii) the free vibration response. In this work, the term *forced vibration response* refers to the dynamic response of the bridge while the human-induced excitation (walking, running, or jumping) is actively applied, whereas the term *free vibration response* denotes the subsequent free decay phase of the bridge once the human excitation ceases (Zivanovic et al. 2005). As an illustrative example, Fig. 5a displays the vertical acceleration time-history measured by accelerometer A4 during Test #4 (see Table 1), where the two responses are clearly identified. The free decay phase of the free vibration response is shown in Fig. 5b.

For each vibration response (i.e. forced or free vibration response, independently), the Power Spectral Density (PSD) has been estimated and averaged in the cases for which several repetitions were measured and therefore available. Note that, in the PSD spectra reported in the following sections, the frequency resolution could be different, since it depends on the length of the considered signal. In this work, it was chosen to be close to that used in the dynamic identification process discussed in Section 4 (namely, 0.01 Hz).

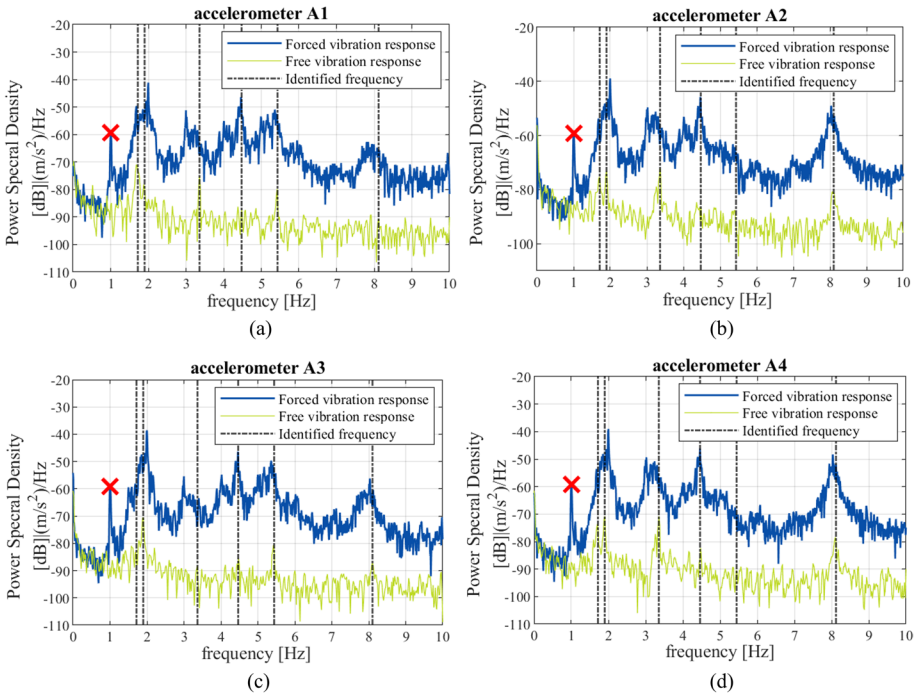

Fig. 6 PSDs of the vibration responses measured during Test #4 (walking of 13 people at 1 Hz): (**a**) accelerometer A1, (**b**) accelerometer A2, (**c**) accelerometer A3, and (**d**) accelerometer A4. In each plot, the red cross indicates the imposed frequency of the walking input

5.1 Walking tests

The walking human-induced tests have been carried out to measure the effects (mostly in terms of acceleration) of both a small (e.g. 3) and a large (e.g. 13) number of people, with reference to the pedestrian bridge at hand. The number of persons (13) composing the large group was selected to meet the requirements of both Section A2.4.3 of Eurocode 0 (EN 1990) (the group should be of about 8 to 15 persons) and the JRC Technical and Scientific Report (Heinemeyer et al. 2009) on the design of lightweight footbridges (the group should include 10 pedestrians for deck widths up to 2.5 m and 15 for wider decks). During the tests, the pacing rate of people walking has been set equal to 1 Hz and 2 Hz, making use of a metronome in order to achieve synchronisation. The 1 Hz frequency was selected for easiness of implementation from the walking group; the 2 Hz frequency was selected since it was similar to the first two identified ones of the footbridge structure (see Table 2), potentially leading to resonance phenomena. Furthermore, both values well fit the critical range for the walking motion highlighted in the scientific literature (1.2–2.4 Hz). Figure 6 reports the PSDs of the two (forced and free) vibration responses measured by the four accelerometers during Test #4 (walking of 13 persons at 1 Hz), together with the identified frequencies reported in Table 2 (purple vertical lines).

Inspection of Fig. 6 allows the following observations:

- The PSD spectra of forced vibration are higher than the ones of free vibration since they have higher energy content.

- The dynamic identification results are confirmed, since the vertical purple lines representing the identified frequencies reported in Table 2 well match the peaks on the free vibration spectra (the green ones).
- The input frequency of the walking motion (pacing rate) is well recognizable from the peaks on the forced vibration spectra (blue curves). For instance, the peaks of the blue curves close to the imposed frequency (identified with a red cross) at 1 Hz confirm that people walking was correctly imposed at 1 Hz during the test.
- In general, a small shift is observed of the bridge natural frequencies as evaluated under the forced response with respect to the ones as evaluated under the free response. In detail, during Test #4, the following shifts (to lower frequency values) for all the sensors are observed: (i) the third mode moves from 3.36 Hz to 3.00 Hz (−11%), (ii) the fifth mode from 5.44 Hz to 5.35 Hz (−2%), (iii) the sixth mode from 8.11 Hz to 8.00 Hz (−1%). The first and fourth modes appear almost stable, while the second mode shows a frequency shift towards slightly higher values, from 1.90 Hz to 2.00 Hz (+5%). The percentage of the frequency shift decreases with increasing mode number. In general, these results might be associated to mass and stiffness variations. Regarding mass, during Test #4, the weight of the 13 people (around 10 kN) is almost 1.1% of the total weight of the pedestrian bridge (930 kN). Consequently, mass variation can be considered negligible in the frequency evaluation. This is also consistent with the recommendation that the mass of pedestrians should be considered when calculating the natural frequencies only when the modal mass of the pedestrians is more than 5% of the modal deck mass (Heinemeyer et al. 2009). Regarding stiffness, a higher input may change the restraint conditions, by activating rotational and longitudinal response at the springings of the arch after exceeding friction forces, which could be inhibited for ambient vibrations. For instance, a roller behaviour of the restraints at the springings (instead of a pinned connection behaviour) reduces the stiffness, thus decreasing the frequency (consistent with all modes except mode n. 2).

As a concluding remark, it has to be observed that in the identification of the bridge's modal properties, supports and boundary conditions have a relevant influence in lighter than heavier structures (Caetano and Cunha 2013), such as the lightweight steel arch pedestrian bridge considered in this work. In the present case, the arch results in a statically indetermined scheme, by being hinged at both extremities at the lower chord level, while the boundary condition of the upper chords supporting the walkway slab are designed to be hinged on one side, and to allow displacements and rotations on the other. However, due to the abutment geometry and the realisation of this connection on site (see Fig. 1c), the upper chord profiles are partially embedded in the abutment. This, indeed, could trigger a frictional contribution in the vibration response depending on the intensity level of the input, which consequently modifies the global stiffness and the modal properties.

5.2 Running tests

Similarly to walking tests, the running tests were carried out with 3 and 10 persons. In this case, the pacing rate of people running has been set equal to 3 Hz, as also suggested

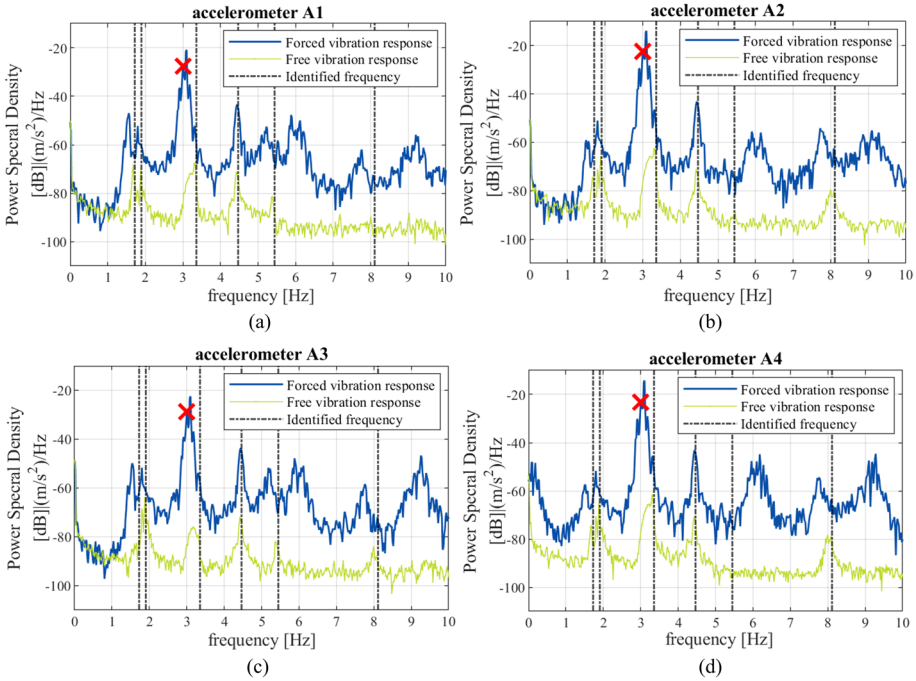

Fig. 7 PSDs of the vibration responses measured during Test #6 (running of 3 people at 3 Hz): (**a**) accelerometer A1, (**b**) accelerometer A2, (**c**) accelerometer A3, and (**d**) accelerometer A4. In each plot, the red cross indicates the imposed frequency of the running input

by Setra (2006). Figure 7 reports the PSDs of the vibration responses measured during Test #6 (running of 3 persons at 3 Hz).

Inspection of Fig. 7 allows observations similar to those provided for the walking motion. Specifically, the input frequency of the running motion (pacing rate) is well recognizable from the peaks on the forced vibration spectra (blue curves). For instance, the peaks at around 3 Hz confirm that people running was quite well imposed at 3 Hz during the test. The slight difference is due to the difficulty in imposing the same pacing rate for all the three people.

5.3 Jumping tests

Analyses of jumping tests have been conducted both in time and frequency domain.

First, Fig. 8 represents the vertical acceleration time-history plot during Test #12 (jumping of 4 people in the accelerometer A2 position). This kind of test is characterised by a first impulsive response (less than 1 s) followed by a free vibration response. This is mainly governed by the first two flexural modes (frequencies slightly lower than 2 Hz), but it also contains several modes contributions (more than one harmonic functions are visually detectable), since the deformed shape of the bridge structure under a concentrated load placed at the jump position does not correspond exclusively to any specific modal shape (structures in free vibration oscillate following the shape of a specific mode only if it is properly activated (Chopra 2012), but in turn it corresponds to the superposition of several modal shapes. From a serviceability point of view, it is worth pointing out that 4 people for a total weight of about 3 kN lead to a peak vertical acceleration value of about 2.3 m/s^2.

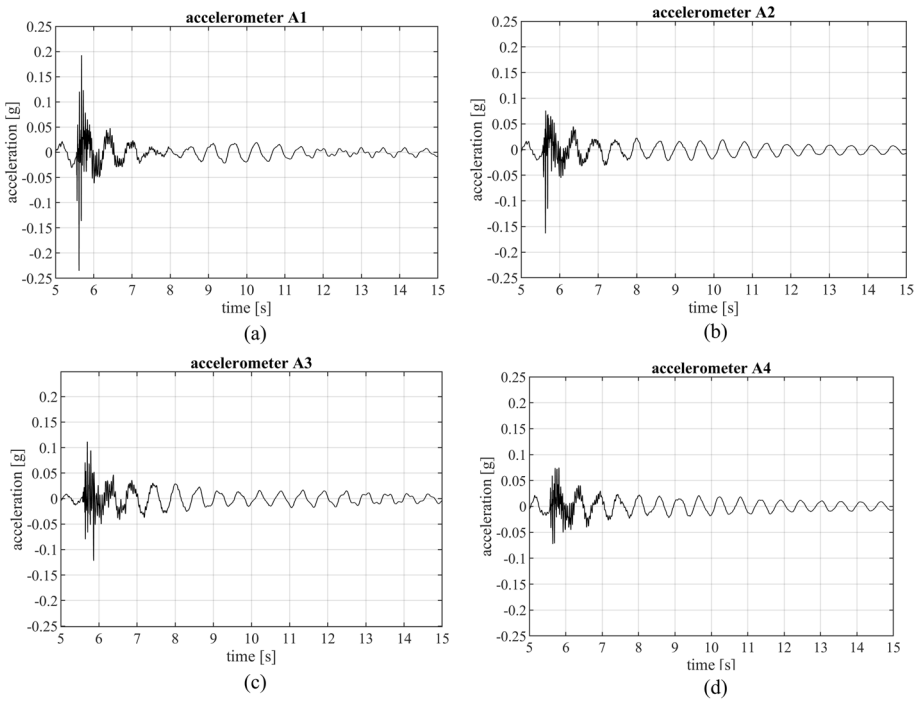

Fig. 8 Vertical accelerations measured during Test #12 (jumping of 4 people in the accelerometer A2 position): (**a**) accelerometer A1, (**b**) accelerometer A2, (**c**) accelerometer A3, and (**d**) accelerometer A4

Second, the PSD of the free vibration response part of the signal is calculated and reported in Fig. 9, which clearly shows a number of modal frequencies that confirm the previous observation regarding the activation and superposition of several modes.

If the raw acceleration time-history registration is then filtered with a pass-band filter centred around the frequency of a given mode, the specific contribution of that mode to the whole response is distilled and the specific damping ratio of that mode can be easily estimated with different techniques, such as fitting of the damped response and logarithmic decrement method (Chopra 2012).

Figure 10 reports the time-history of the accelerometers A1 and A3 after the filtering with a band around the first mode frequency. The figure also displays the peaks of the response and their exponential fit in a selected time range (7.5 –25 s). The range has been selected in such a way that enough free response is taken into account in the damping ratio estimation.

For each accelerometer, for the i-th mode, the exponential best fit has been assumed as:

$$y(t) = C_i \cdot e^{-\xi_i \cdot 2\pi \cdot f_i \cdot t} \tag{1}$$

where, on one hand, $y(t)$ and f_i are the time-history response (in this case: vertical acceleration) and the vibration frequency of the i-th mode, respectively. On the other hand, C_i and ξ_i represent a constant and the i-th modal damping ratio to be determined in the best fitting operation, respectively. The application of Eq. (1) to the response reported in Fig. 10 gives damping ratio values equal to 2.98% and 3.44%, for accelerometers A1 and A3, respectively. Similarly, the same approach has been applied to different modes

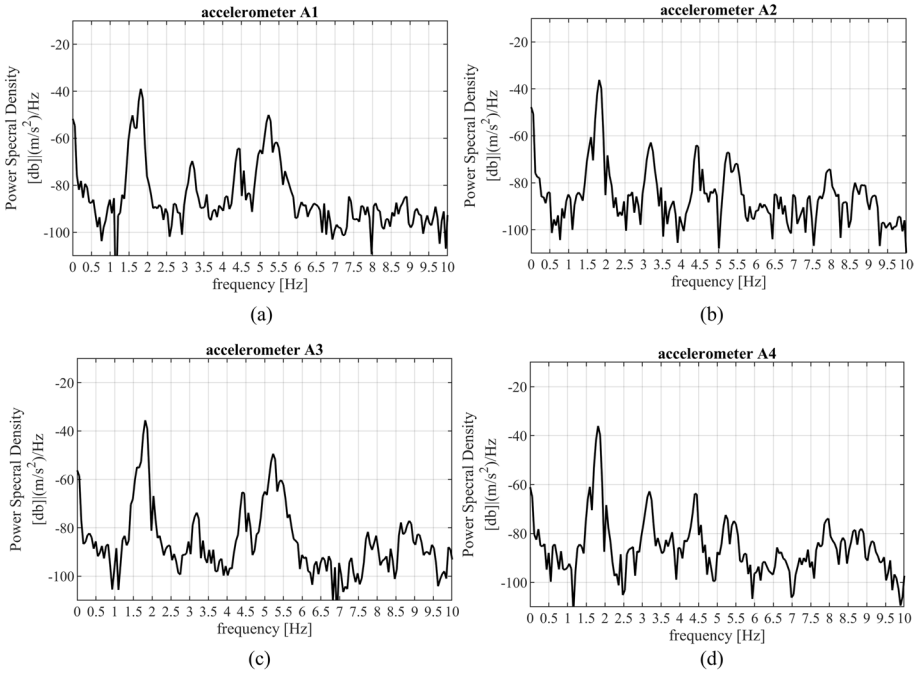

Fig. 9 PSDs of the free vibration response measured during Test #12 (jumping of 4 people in the accelerometer A2 position): (**a**) accelerometer A1, (**b**) accelerometer A2, (**c**) accelerometer A3, and (**d**) accelerometer A4

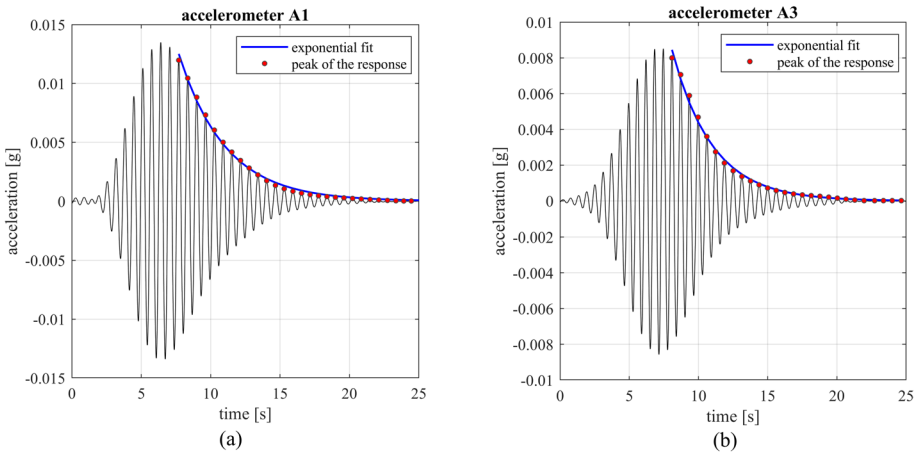

Fig. 10 Time-history acceleration of the accelerometer A1 (**a**) and A3 (**b**) after the filtering with a band around the first mode during Test #12 together with the exponential fit of the free vibration phase

(through application of specific frequency bands) and for different jumping tests. Table 3 reports the mean value of the damping ratios obtained only for the accelerometers, whose free vibration response proved to be reliable within this context (they can vary from a test to another one, as highlighted in the last column of the table).

The same approach has been used in the application of the logarithmic decrement method. It has been applied taking advantage of the first and the last of the identified

Table 3 Damping ratios estimated through the exponential fit of the free vibration response

Test number	Damping ratio [%]			Reliable accelerometers
	Mode 1	Mode 2	Mode 3	
10	3.75			A1, A3
		1.44		A1, A2, A3, A4
			2.60	A1, A2, A3, A4
12	3.23			A1, A3
		1.32		A2, A3, A4
			1.88	A1, A2, A3, A4
17	3.40			A1, A3
		1.36		A2, A4
			-	

Table 4 Damping ratios estimated through the logarithmic decrement of the free vibration response

Test number	Damping ratio [%]			Reliable accelerometers
	Mode 1	Mode 2	Mode 3	
10	3.44			A1, A3
		1.39		A1, A2, A3, A4
			4.52	A1, A2, A3, A4
12	3.07			A1, A3
		1.22		A2, A3, A4
			3.76	A1, A2, A3, A4
17	2.75			A1, A3
		1.21		A2, A4
			-	

peaks in the selected free vibration response measured in the considered time range. It leads to the damping ratios reported in Table 4.

The results reported in Tables 3 and 4 show that the first three modes have damping ratios in the range 2–4%, which are perfectly in line with the values provided in Table 4.6 by Heinemeyer et al. (2009) for large vibrations (intentional loading such as jumping) in pedestrian steel bridges, and also with the typical values of damping ratio for light steel structures (Chopra 2012). The damping ratios calculated by means of the logarithmic decrement method are lower than the ones obtained by the application of Eq. (1) for the first two modes, whilst they are higher for the third mode. It is worth noting that both the techniques provide an estimation of the modal damping ratios: the first one as the result of a fitting operation conducted on selected (more than two) peaks of the acceleration time-history, and the second one by using only two peaks of the acceleration time-history. A comparison with the results reported in Section 4 demonstrates that the damping ratios obtained through the OMA technique (specifically by EFDD on data elaborated from ambient vibration tests) result underestimated, confirming that the damping measurement is difficult to be precise and repeatable (Rainieri and Fabbrocino 2014) and that damping ratios may strongly depend on the level of oscillation, as also recognised by Heinemeyer et al. (2009). Indeed, the different level of oscillation and the

nature of the excitation are among the factors that may introduce variability in the evaluation of damping ratio values. EFDD, based on spectral density estimation, tends to provide stable values under broadband excitation; this method is thus less sensitive to noise (Brincker and Ventura 2015). However, especially for steel structures, it may lead to the underestimation of damping ratios (Hasan et al. 2018). On the contrary, the logarithmic decrement and the exponential fit methods are applied to the data of the free vibration response in human-induced vibration tests, and, since they are time-domain methods resulting in straightforward and computationally cost-effective procedures, they are also more prone to overestimate or underestimate damping in the presence of noise (Casiano 2016). Moreover, while the logarithmic decrement method assumes a purely exponential decay, the exponential fit method may improve the approximation of the free decay phase by interpolating more peaks of the response, but it is then more sensitive to the quality of the considered free-decay phase segments. Consequently, the damping ratio values obtained with EFDD under ambient vibration and the ones obtained with time-domain methods for the decay phase after human-induced excitation should be interpreted as complementary references (representing different test conditions) for further comparison, rather than strictly overlapping. Furthermore, it has to be observed that the damping ratio values obtained with these methods are derived under the assumption that the signal is dominated by a single, lightly damped mode. Consequently, their reliability decreases when multiple modes contribute significantly and are not clearly separated. Nevertheless, the accuracy of the estimation can be improved if a dominant mode is present or if modal contributions are isolated, for instance by applying a band-pass filter, as illustrated in Fig. 10.

In conclusion, the damping ratios obtained in ambient vibration (Section 4) match the values of Table 4.5 by Heinemeyer et al. (2009), whilst the damping ratios obtained in after-jump vibration (this Section 5.3) match the values of Table 4.6 by Heinemeyer et al. (2009) and are thus comparable with earthquake effects.

5.4 Acceptance criteria

As described in the introduction, acceptance criteria for footbridges are related to the pedestrian comfort. In detail, the following ranges can be assumed as acceptable for 1 Hz human-induced vertical motion: (i) 0.5–1.0 m/s^2 and 0.2–0.4 m/s^2 for vertical and lateral motion, respectively (Dallard et al. 2001), (ii) 1.0–2.5 m/s^2, being the latter value the unacceptable discomfort limit (Heinemeyer et al. 2009), and (iii) 0.7 m/s^2 (EN 1990). For 2 Hz human-induced vertical motion, the range 0.5–0.8 m/s^2 (Setra 2006) can be assumed as acceptable. Table 5 reports the maximum acceleration values measured during the walking and running tests by the four accelerometers together with the above-mentioned acceptance limit values.

The values reported in Table 5 highlight that walking tests (#3, #4 and #5) are characterized by acceleration peak values that are in the range of the widely adopted acceptance criteria for SLS. On the contrary, the running tests lead to peak acceleration values out of the range of the acceptance criteria for SLS as per Setra (2006), Heinemeyer et al. (2009), and Dallard et al. (2001) assuming the lower bound of the range. The discomfort acceleration level (2.5 m/s^2) considered unacceptable by Heinemeyer et al. (2009) has never been achieved during the tests. The limit (0.7 m/s^2) provided by the Eurocode 0 turned

Table 5 Comparison between the measured peak accelerations with the limits provided by codes

Test type	Test number	People number	Measured peak accelerations [m/s^2]				Eurocode 0 (Dallard et al. 2001) limit [m/s^2]	(EN 1990) limit [m/s^2]	(Caetano et al. 2009) limits [m/s^2] (comfort classes)	Setra (Bachmann and Walter 1987) limit [m/s^2]
			A1	A2	A3	A4				
Walking	3	3	0.20	0.25	0.28	0.27	0.7	0.5–1	<0.5 (maximum comfort) 0.5–1.0 (medium comfort) 1.0–2.5 (minimum comfort)	0.5–0.8
	4	13	0.17	0.14	0.16	0.18				
	5	13	0.35	0.41	0.43	0.43				
Running	6	3	0.59	1.16	0.54	0.72				
	7	10	0.93	1.55	0.95	0.74				

out to be an effective upper bound for walking activities, while it was overcome by accelerometers A2 and A4 for running activities, namely in Test #6 (running of 3 people at 2 Hz) and by all the accelerometers in Test #7 (running of 10 people at 3 Hz). This finding highlights the relevance of incorporating comfort verifications at the design stage of pedestrian bridges, even in regulatory contexts such as Italy, where current standards may not strictly require them.

In fact, although the high vertical accelerations observed in the case study do not compromise the structural safety of the bridge, they highlight potential issues related to pedestrian comfort. In similar situations, the adoption of vibration mitigation devices could be recommended to limit excessive responses and improve user experience. Among the most common strategies, successful applications of tuned mass dampers for vibration control in steel footbridges are reported in the literature from both analytical and numerical points of view (Jiménez-Alonso et al. 2021), in experimental works (Wang et al. 2019; Alhassan et al. 2020), or through design-oriented studies (Caetano et al. 2010b; Caetano and Cunha 2013). Other studies have demonstrated the effectiveness of different typologies of fluid viscous dampers applied to pedestrian footbridges showing high resonant phenomena (Duflot and Taylor 2008; Alhasa et al. 2023). For the present case study, future work could include numerical or experimental investigations on the implementation of such devices, which may prove beneficial for promoting their wider use in the design of pedestrian bridges.

6 Conclusions

In this research work, an example of vibration tests conducted on a case-study of a steel two-hinged arch footbridge with tapered truss cross-section is presented. The dynamic response under environmental and human-induced input was measured by four accelerometers installed on the bridge deck, in order to provide reference orders of magnitude of the deck acceleration responses of a typical steel footbridge. The main results of the experimental tests are summarised hereafter and may act as reference and as practical indications for researchers and practitioners tackling similar problems:

- From the ambient vibration measurements, the first six vibration modes of the bridge are identified in terms of both frequencies and modal shapes, by means of the Frequency Domain Decomposition (FDD) technique. Instead, the damping ratios are estimated using the Enhanced Frequency Domain Decomposition (EFDD) technique. They are all around 1%, in line with the typical values of light steel pedestrian bridges under light excitation. In this regard, it should be noted that the adoption of these identification techniques allows the results to be directly compared with a large body of existing studies on footbridges, which often employ the same methodologies.
- The analyses of the human-induced vibrations, including walking, running and jumping, highlight that the pacing rate of the input was correctly imposed during the tests (as verified ex-post in the PSD plots) and that a small shift is observed of the bridge natural frequencies as evaluated under the forced response with respect to the ones as evaluated under the free response. Rather than being an effect of significant pace asynchrony, the observed shift may be due to a reduction of the rotational

and longitudinal stiffness of the restraints at the springings of the arch, moving from environmental to man-induced loading condition.

- For the jumping tests, the damping ratios are estimated by focusing on the free vibration response after the jump and isolating specific modal responses, through the exponential regression of the time-history response and through the logarithmic decrement method. They are in the range of 2–4%, which are in line with the typical values of light steel pedestrian bridges under severe excitation. The damping ratios are higher than those obtained for environmental vibrations (with EFDD), confirming that they strongly depend on the level of oscillation.
- Consistent with amplitude dependence—particularly for lightweight steel deck-arch footbridges—the damping ratios identified under ambient (OMA) testing are lower (≈1% by EFDD) and should be regarded as a conservative, potentially underestimating baseline. By contrast, free-decay estimates after walking, running or jumping are higher (≈2–4%), likely reflecting additional dissipative mechanisms activated at larger response amplitudes (e.g., interface friction, micro-impacts, hysteresis, boundary condition interactions).
- Finally, the maximum values of the accelerations around the mid-point location of the deck during the walking tests (around 0.45 m/s^2) did not exceed the Serviceability Limit State acceptance criteria limit provided by Eurocode 0 (0.70 m/s^2). On the contrary, during the running tests, they exceeded (1.0–1.5 m/s^2) the same Eurocode 0 limit, but they were in line with other limits provided in the scientific literature.

The present study discusses the experimental identification of modal parameters for a specific bridge typology (two-hinged arch footbridge with tapered truss cross-section), which has remained unaddressed in the state of the art of steel pedestrian bridges. Thus, inheriting some limitations due to the bridge's peculiarities affecting in terms of span, mass and stiffness, the considered case study is representative of an easily implementable design solution for ordinary pedestrian steel bridges with medium-size spans. Given that the structural scheme and the support conditions play a key role in the behaviour of arch bridges, this study emphasizes that experimental results may be affected by case-specificity observed in the actual supports. In this regard, the results obtained in the identification of the modal parameters with reference to the dynamic response of the bridge to different excitations provide an initial benchmark set of values for preliminary analysis and calibration, that would surely benefit from the comparison with further experimental tests performed on similar case studies.

Acknowledgements
Eng. Friedrich Drollmann is gratefully acknowledged for providing technical information about the structural design of the pedestrian bridge. The authors are also grateful to Dr. Mirco Tarozzi for his technical contribution and support for the experimental campaign.

Authors' contributions
MM processed and analysed the experimental data, including the identification of modal parameters. EG contributed to the interpretation of the results and to the drafting of the manuscript. GG conceived the experimental campaign and supervised execution of the dynamic tests on site. SS was responsible for the design and interpretation of the experimental tests and supervised the overall study. All authors discussed the results, contributed to the final version of the paper, and approved the submitted manuscript.

Funding
No funding was received for the current study.

Data availability
Data will be made available from the corresponding author upon reasonable request.

Declarations

Competing interests
The authors report there are no competing interests to declare.

Received: 18 July 2025 Revised: 22 September 2025 Accepted: 14 October 2025
Published online: 04 January 2026

References

Alhasa AA, Vafaei M, Ali SC, Jian TW (2023) Viscoelastic damper for vibration mitigation of footbridges. In IOP Conference Series: Earth and Environmental Science, vol 1205, no 1. IOP Publishing, p 012051. https://doi.org/10.1088/1755-1315/1205/1/012051
Alhassan MA, Al-Rousan RZ, Al-Khasawneh SI (2020) Control of vibrations of common pedestrian bridges in Jordan using tuned mass dampers. Procedia Manuf 44:36–43
Bachmann H, Ammann W, (1987) Vibrations in structures: induced by man and machines. (Vol 3) International Association for Bridge and Structural Engineering, Zurich, Switzerland.
Banerjee S, Saravanan TJ (2024) Utilizing data-driven algorithms for blind modal parameter identification of structures from output-only video measurements. In: Structures, vol 63. Elsevier, p 106410. https://doi.org/10.1016/j.istruc.2024.106410
Barbosa R, Magalhães F, Caetano E, Cunha A (2013) The Viana footbridge: construction and dynamic monitoring. Proceedings of the Institution of Civil Engineers-Bridge Engineering 166(4):273–290
Brincker R, Zhang L, Andersen P (2000) Modal identification from ambient responses using frequency domain decomposition. IMAC 18: Proceedings of the International Modal Analysis Conference, San Antonio, Texas, USA, 625–630 February 2000
Brincker R, Ventura CE, Andersen P (2001) Damping estimation by frequency domain decomposition. In Proceedings of IMAC 19: A conference on structural dynamics: February 5–8, 2001, Hyatt Orlando, Kissimmee, Florida, 2001 (pp. 698–703). Society for Experimental Mechanics
Brincker R, Ventura C, Andersen P (2003) Why output-only modal testing is a desirable tool for a wide range of practical applications. In: Proceedings of the International Modal Analysis Conference (IMAC) 21: A Conference on Structural Dynamics. pp 265–272
Brincker R, Ventura C (2015) Introduction to operational modal analysis. John Wiley & Sons, Chichester, United Kingdom
Caetano E, Cunha A, Magalhães F, Moutinho C (2010a) Studies for controlling human-induced vibration of the Pedro e Inês footbridge, Portugal. Part 1: assessment of dynamic behavior. Eng Struct 32(4):1069–1081
Caetano E, Cunha A, Magalhães F, Moutinho C (2010b) Studies for controlling human-induced vibration of the Pedro e Inês footbridge, Portugal. Part 2: implementation of tuned mass dampers. Eng Struct 32(4):1082–1091
Caetano E, Cunha A (2013) Implementation of a passive control system in a lively footbridge. In: IABSE Symp Rep vol 99, no 20. pp 760–767
Caetano E, Cunha A, Hoorpah W, Raoul J (2009) Footbridge Vibration Design. 1st Edition. Taylor & Francis Group. London, United Kingdom. https://doi.org/10.1201/9781482266511
Casiano MJ (2016) Extracting damping ratio from dynamic data and numerical solutions No M-1418
Chopra AK (2012) Dynamics of structures : theory and applications to earthquake engineering, 4/E. https://www.pearson.com/us/higher-education/product/Chopra-Dynamics-of-Structures-4th-Edition/9780132858038.html
Cunha A, Caetano E, Magalhães F, Moutinho C (2013) Recent perspectives in dynamic testing and monitoring of bridges. Struct Control Health Monit 20(6):853–877
Da Silva IAR, Da Silva JGS (2018) Experimental and numerical dynamic structural analysis of footbridges when subjected to pedestrians walking loads. J Civ Struct Health Monit 8(4):585–595
Dallard P, Fitzpatrick T, Flint A, Low A, Smith RR, Willford M, Roche M (2001) London Millennium Bridge: pedestrian-induced lateral vibration. J Bridge Eng 6(6):412–417
Duflot P, Taylor D (2008) Fluid viscous dampers: an effective way to suppress pedestrian-induced motions in footbridges. In Third International Conference: Footbridge
EN 1990, 2002. (2002). Eurocode - Basis of structural design. Eurocode 0
Feng K, Hester D, Taylor S, O'Higgins C, Ferguson A, Zhu Z, Zou G, Lydon M, Early J (2024) Experimental modal identification of a pedestrian bridge through drive-by monitoring integrated with shared-mobility vehicles. Dev Built Environ 20:100562
Hajdu Robert (2014) Brücken im Phoenix-Park in Dortmund. Entwurf und Realisierung einer »Brückenfamilie«. In: Brückenbau, vol 6, no 6. pp. 6–12
Hasan AMD, Ahmad ZAB, Salman Leong M, Hee LM (2018) Enhanced frequency domain decomposition algorithm: a review of a recent development for unbiased damping ratio estimates. J Vibroeng 20(5):1919–1936
Heinemeyer C, Martin P-O, Trometor S, Keil A, Cunha A, Lukic M, Lemaire A, Butz C, Chabrolin B, Caetano E (2009) Design of Lightweight Footbridges for Human Induced Vibrations: Background document in support to the implementation, harmonization and further development of the Eurocodes; Joint Report, prepared under the JRC-ECCS cooperation agreement for the evolution of Eurocode 3 (programme of CEN/TC 250) (No.

RWTH-CONV-009271). Lehrstuhl für Stahl-und Leichtmetallbau und Institut für Stahlbau. Office for Official Publications of the European Communities, Luxembourg
Jiménez-Alonso JF, Soria JM, Díaz IM, Guillen-Gonzalez F (2021) A common framework for the robust design of tuned mass damper techniques to mitigate pedestrian-induced vibrations in lively footbridges. In Structures vol 34. Elsevier, pp 1276–1290. https://doi.org/10.1016/j.istruc.2021.08.070
Li Y, Zhang X, Wang C, Zhang Y, Wei X (2023) Human-induced vertical vibration of a glass suspension footbridge: experimental study and numerical analysis. Struct Infrastruct Eng 0(0):1–19. https://doi.org/10.1080/15732479.2023.2230567
Maraveas C, Fasoulakis Z, Tsavdaridis K (2015) A review of human induced vibrations on footbridges. Am J Eng Appl Sci 8(4):422–433. https://doi.org/10.3844/ajeassp.2015.422.433
NTC 2018 (2018) Norme tecniche per le costruzioni. DM 17/1/2018. In: Gazzetta Ufficiale della Repubblica Italiana, vol 20. https://www.gazzettaufficiale.it/eli/gu/2018/02/20/42/so/8/sg/pdf
Peeters B (2000) System identification and damage detection in civil engineering. Dissertation, Katholike Universite Leuven, Belgium
Peeters B, De Roeck G (1999) Reference-based stochastic subspace identification for output-only modal analysis. Mech Syst Signal Process 13(6):855–878
Quqa S, Giordano PF, Limongelli MP (2022) Shared micromobility-driven modal identification of urban bridges. Autom Constr 134:104048
Racic V, Pavic A, Brownjohn JMW (2009) Experimental identification and analytical modelling of human walking forces: literature review. J Sound Vib 326:1–49
Rainieri C, Fabbrocino G (2014) Operational modal analysis of civil engineering structures: an introduction and guide for applications. Springer, New York, pp 142–143
Setra AFGC (2006) Footbridges. Assessment of vibrational behaviour of footbridges under pedestrian loading. Technical guide SETRA, Paris, France.
Shahabpoor E, Pavic A, Racic V (2016) Interaction between walking humans and structures in vertical direction: a literature review. Shock Vib 1:3430285
Van Nimmen K, Lombaert G, De Roeck G, Van den Broeck P (2014) Vibration serviceability of footbridges: evaluation of the current codes of practice. Eng Struct 59:448–461
Van Nimmen K, Van Hauwermeiren J, Van den Broeck P (2021) Eeklo Footbridge: Benchmark Dataset on Pedestrian-Induced Vibrations. J Bridg Eng 26(7):1–17
Wang D, Wu C, Zhang Y, Li S (2019) Study on vertical vibration control of long-span steel footbridge with tuned mass dampers under pedestrian excitation. J Constr Steel Res 154:84–98
Welch P (1967) The use of fast Fourier transform for the estimation of power spectra: a method based on time averaging over short, modified periodograms. IEEE Trans Audio Electroacoust 15(2):70–73
Wirsching PH, Paez TL, Ortiz K (2006) Random vibrations: theory and practice. Courier Corporation. John Wiley & Sons. New York, United States.
Zivanovic S, Pavic A, Reynolds P (2005) Vibration serviceability of footbridges under human-induced excitation: a literature review. J Sound Vib 279:1–74

Publisher's Note